Electrochemical Behavior of Titanium Thin Films Obtained by Magnetron Sputtering

David TURCIO-ORTEGA*, Sandra Elizabeth RODIL, Stephen MUHL

Instituto de Investigaciones en Materiales, Universidad Nacional Autónoma de México,
Ciudad Universitaria, 04510 México D. F., México

A study of titanium thin films deposited on stainless steel 316L having different thickness was carried out using the Electrochemical Impedance Spectroscopy (EIS) and Polarization Curves (PC) experiments as the coated system were immersed in 0.89 % NaCl solution. The interpretation of the EIS data is based upon a two-layer model of the film, consisting of a Ti thin film and a Ti-oxide outer layer. The circuit parameters were correlated with the dielectric characteristics and microstucture of the titanium thin films. Analysis of experimental results done by modelling the EIS data show that the corrosion process was getting difficult with time, while the PC gives information about the corrosion rate of the coated systems as a function of the thickness of the Ti deposit.
Keywords: titanium thin films; magnetron sputtering; biomaterials; EIS.

INTRODUCTION

Titanium has attracted considerable interest in aerospace, chemical processes, and in biomedical industries; due to the good mechanical properties, excelent corrosion resistance and good biocompatibility. The chemical stability of titanium results the presence of a thin but stable surface oxide film, typically a few nanometers thick [1].

Titanium thin films have many potential applications such as the buffered layer to serve as a "bond" coat for coatings like amorphous carbon on stainless steel [2], as "dry" active electrodes in electroencephalographic studies [3], or as a biomaterial, because it has high tensile strenght and low modulous of elasticity: after implantation it provides a favourable body reaction that leads to mineralization and titanium osseointegration [4].

Film deposition by magnetron sputtering (MS) offers special advantages as high deposition rates, high density films, and good adhesion to the stainless steel substrate [5].

The purpose of this paper is to analyze the electrochemical behavior of stainless steel coated with Ti thin films of different thicknesses in 0.89 % NaCl obtained by MS.

EXPERIMENTAL PROCEDURE

The AISI 316L stainless steel (SS) sheets were cut into square pieces of 1 cm × 1 cm size. The substrates were polished with SiC 600 and then cleaned using ultrasonic cleaner, first in acetone, and then in dionized (DI) water.

The titanium thin films of different thickness were deposited directly on the SS substrates using a MS system and a DC-pulsed argon plasma as shown in Figure 1.

Firstly, the vacuum chamber was evacuated by a turbo pump coupled with a mechanical pump, until a residual pressure below 1×10^{-5} Torr. Then, 10 sccm of argon (99.99 %) were added to get a processing pressure of

4 mTorr. The water-cooled titanium target worked as the cathode of the glow discharge, and the anode was the grounded chamber. The power generated was 250 W (watts) and the pulsed frequency was 250 kHz.

1 Deposition Chamber
2 Magnetron Head
3 Titanium target
4 Shutter
5 Sample Holder
6 Flowmeter
7 DC Source
8 Cooling System
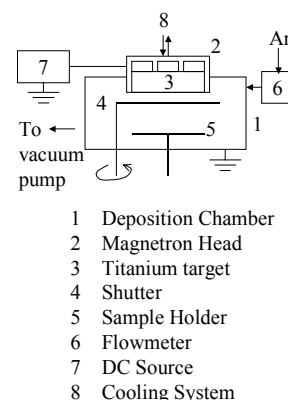
Fig. 1. Schematic representation of MS arrangement

Electrochemical experiments were carried out with a standard three-electrode system as it is shown in Figure 2. A saturated calomel electrode (SCE) was used as the reference electrode with a platinum counter electrode. The working electrode was served the Ti coated stainless steel. The electrolyte was a solution of 0.89 % NaCl, pH 7.4. Tests were performed at room temperature, under static conditions and the solution was open to the air. EIS experiments were carried out as a function of the immersion time, up to 195 h. The frequency range of 10 kHz to 1 mHz was used. Five data points per decade were measured at amplitude of 30 mV. Polarization curves were obtained after the EIS experiments, the scan rate was 0.1666 mV/sec from the initial potential of -0.28 mV versus the Open Circuit Potential (OCP) to the final potential of 0.28 mV.

Electrochemical experiments were done using the Gamry electrochemical unit Framework 2004. EIS data were interpreted on the basis of the equivalent circuit model and the parameters were obtained by the Levenberg-

---

*Corresponding author. Tel.: +52-55-56224734; fax.: +52-55-56161251.
E-mail address: *dturcio@hotmail.com* (D. Turcio-Ortega)

Marquardt non-linear least square fitting method provided by the Echem-Analyst software.
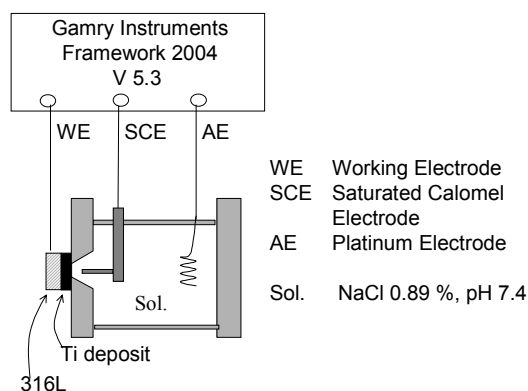
Fig. 2. Schematic diagram showing the arrangement of the electrochemical cell

The microstructures of the deposits were investigated with scanning electron microscopy (SEM) from Leica, Cambridge, mod. Stereoscan 44, and the elements present were identified by energy dispersive spectroscopy (EDS) with a Pentafet detector (Oxford). The coated samples were analyzed with a Profilometer Dektak II in order to measure the thickness of the deposits.

RESULTS AND DISCUSSIONS

Table 1 shows the results of the thickness obtained by MS technique at the various time of deposition, the presence of the Ti on the SS was confirmed by EDS. Electrochemical observations included the monitoring of the OCP with time; this is a parameter determined by the rate of cathodic reaction and anodic reaction of a corroding device and, the rates of both reactions depends on the corrosion media and on the chemical composition of electrode material [6].

Table 1. Samples obtained by MS deposition

Sample	Deposition time, s	Thickness, nm
SS	–	-
Ti 100	50	100
Ti 530	300	530

Figure 3 shows the dependence of the OCP with immersion time. As it can be seen, the difference between the OCP for bare and coated substrate samples could reach 0.1 V. The changes of the OCP in time for the sample Ti 100 can be explained by an increase of the anodic activity until 150 h of exposition in the saline solution probably due to some processes of thinning. The OCP values for the sample Ti 530 increased with immersion time with good stability for long term, this behavior can be related with a more compact, defect-free film compared with the Ti 100 sample. SS shows a decrease in the OCP values, which can be associated to the pitting attack and oxide dissolution taking place at the surface.

Figure 4 shows the Nyquist plot and the Bode diagrams of the Ti 100 sample after immersion of 51, 123, 147, 171 and 195 h in the NaCl 0.89 % solution. At high frequencies (10^4 Hz) the absolute impedance curve is almost independent of the frequency, this value represent the electrolyte resistance, as is shown in the magnitud-Bode plot. Two time constants can be distinguished in the phase diagram in all cases. The first time constant is observed at 10^0 Hz and it is attributed to the oxide electric capacitance of the titanium thin film while the second time constant at low frequencies takes account of the slight titanium dissolution in the presence of the saline solution.
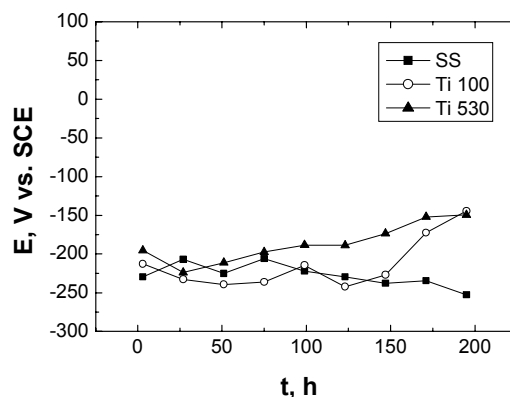
Fig. 3. OCP values of the samples as a function of immersion time

The evolution of the EIS spectra for the sample Ti 530 as a function of immersion time is reported in Figure 5 at the Nyquist and Bode plots. The EIS spectra are almost the same than those of Figure 4, showing the presence of two time constants, but the second time constant takes higher values of the phase angle at low frequencies compared to the Ti 100 sample. A comparison of the Nyquist spectra shown in Figures 4 – 5 indicated that the corrosion resistance of both samples increase with immersion time up to 195 h, but higher values of impedance at low frequencies are observed for the sample Ti 530, suggesting that the Ti-oxide passive layer in combination with the low porosity make difficult the corrosion process, while for the sample Ti 100 the main disadvantage is the high porosity, as is evident with the low impedance values in the real part of the Nyquist diagram for the first 171 h.

The physical model for the coated samples is illustrated in Figure 6, a, which consist of an outer layer of titanium oxide and an inner layer of titanium deposited on the SS. This model considers that the steel substrate is exposed to the electrolyte through permeable defects, like for example pores in the Ti film obtained by MS.

In Figures 4 and 5, the experimental data are shown by symbols and the simulated data by dashed lines. The simulation was obtained using the electric equivalent circuit (EEC) shown in Figure 6, b, where R_s corresponds to the solution resistance, R_1 is the pore resistance, R_2 is the substrate polarisation resistance, C_1 is the coating capacitance and C_2 is the substrate capacitance.

Constant phase elements (CPE) were used instead of pure capacitors because the semicircles in the Nyquist plots are depressed due to surface roughness, heterogeneity of the surface, or other effects that causes uneven current distributions on the electrode surface [7]. Good agreement was observed between the simulated and the experimental data in Figures 4 and 5.
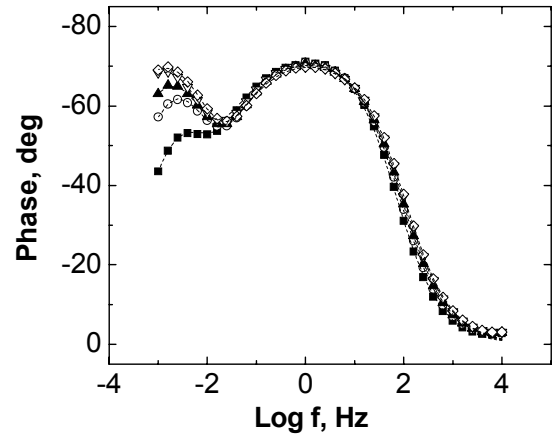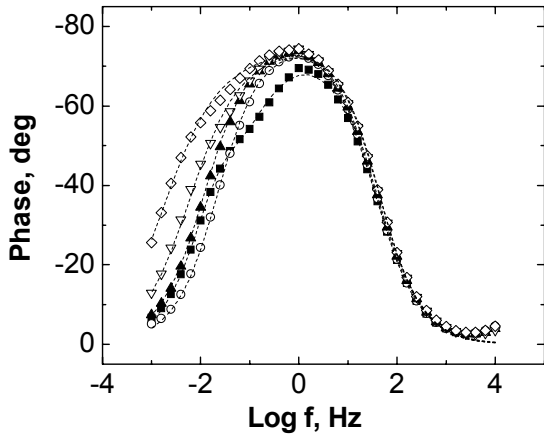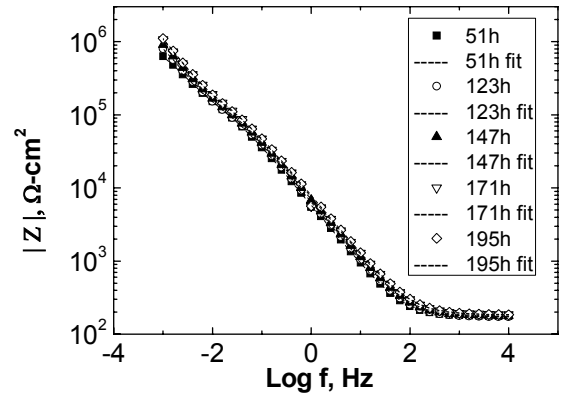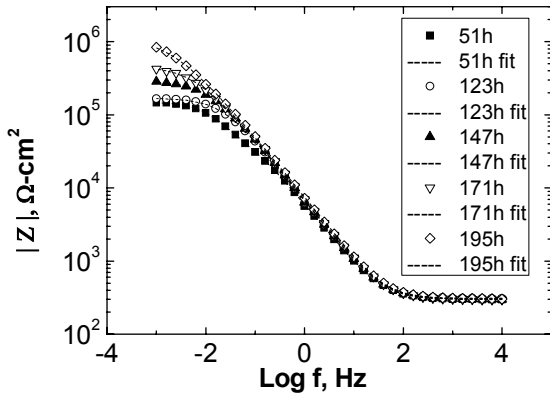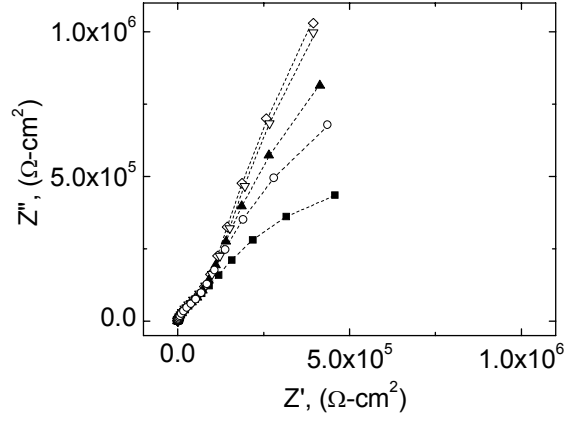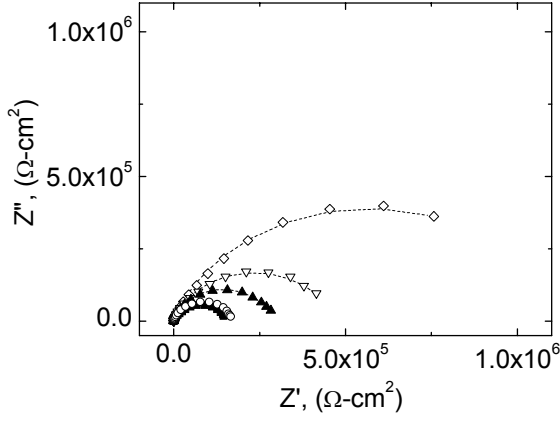
Fig. 4. Nyquist and Bode plots of the experimental data for Ti 100 and simulated spectra according to the model of Fig. 6, a

Fig. 5. Nyquist and Bode plots of the experimental data for Ti 530 and simulated spectra according to the model of Fig. 6, a

Figure 7 shows the impedance spectra of the bare substrate and its evolution in time. The EEC proposed for SS after a long period of exposure to the saline solution should take in consideration the presence of a passive film which has different behavior of a thin film obtrained by MS. We introduce the EIS data of SS in order to compare the behavior of the bare metal with the coated systems by the use of the same electric circuit; R_1 and C_1 are correlated to the metal film interface and, R_2 and C_2 to the redox process taking place in the passive layer.

Table 2 lists the fitting parameters from the modelling of the EIS data by the use of the EEC from Figure 6, b, for the Ti 100, Ti 530 and SS samples. The impedance of a CPE is defined as:

$$\frac{1}{Z_{CPE}} = Q*(j\omega)^n \tag{1}$$

where Z_{CPE} is the impedance of the CPE, Q is a proportional factor, ω is the angular frequency, and n is a factor which represent the non-ideality (if n is equal to 1

then we have an ideal capacitor) [7, 8]. The R_2 values for SS are changing with time; this is probably related to the pitting attack and oxide disolution at the surface.
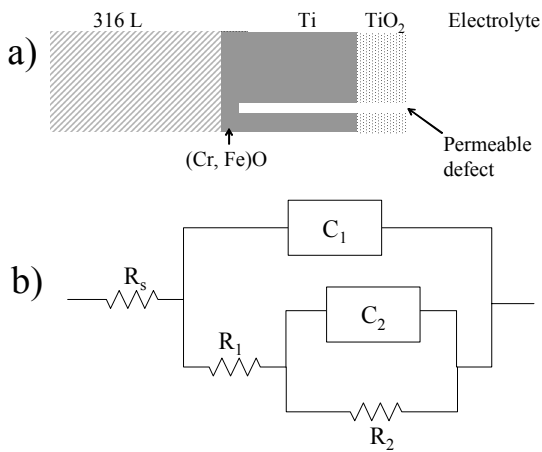
Fig. 6. a – Schematic representation of the Ti deposit, b – EEC used in the generation of the simulated data

The low values of R_2 for the Ti 100 sample below the 123 h can be attributed to some processes of thinning but, an increase of this value at 195 h could be related with the slow growth of a new oxide layer. The Ti 530 sample displayed higher R_2 values which can be compared with those obtained between 8 MΩcm^2 and 22 MΩcm^2 by other authors [3, 9]. The high values of R_2 can be related to the blocking character of the Ti-TiO$_2$ layers with the advantage of a low content of permeable defects compared with the sample Ti 100.

The R_1 values for the Ti 100 sample decreased with time while for the Ti 530 sample these values were between 198 kΩcm^2 and 254 kΩcm^2; these results suggest a better performance of the Ti-TiO$_2$ bilayer with a slight decrease in the C_1 values. The Q_2 values show a decrease with time for both coated samples which can be related to the slow growth of titanium oxide film. This is an indication of the long term stability of the passive film in the NaCl solution.

The polarization curves of the uncoated, and Ti-coated samples are shown in Figure 8. The straight line segments of these scans are identified by the Tafel equation:

$$\Delta E = b \log\left(\frac{i}{i_0}\right) \qquad (2)$$

where b is a constant and, i_0 is the exchange current density. The expanded form of this equation shows linearity where b is slope and $\log i_0$ is the Y intercept. In this case the term "i_0" corresponds to the corrosion current density "i_{corr}". The results of the Tafel extrapolation are summarized in Table 3.

It can be revealed from the parameters obtained that the measured corrosion potential (E_{corr}) has a more positive value only for the Ti 530 sample. Although, not very evident from the figure (Fig. 8) there was a lower corrosion current density (i_{corr}) for both coated samples showing values of 28.1 nA/cm^2 and 18.9 nA/cm^2 for the Ti 100 and Ti 530 samples, respectively, compared to the higher i_{corr} of 60 nA/cm^2 from the SS. These results are in agreement with the values obtained by other researches [10, 11]. In a

much smaller potential range, typically ±10 mV to the E_{corr} value, the slope of the linear segment of the ΔE vs. Δi plot is expressed by the formula [12]:

$$\left(\frac{\Delta E}{\Delta i}\right)_{E \to 0} = R_p = \frac{B}{i_{corr}} \qquad (3)$$

where R_p is the polarization resistance, also reported in Table 3. These results indicate that the Ti 530 sample has the highest value of R_p.
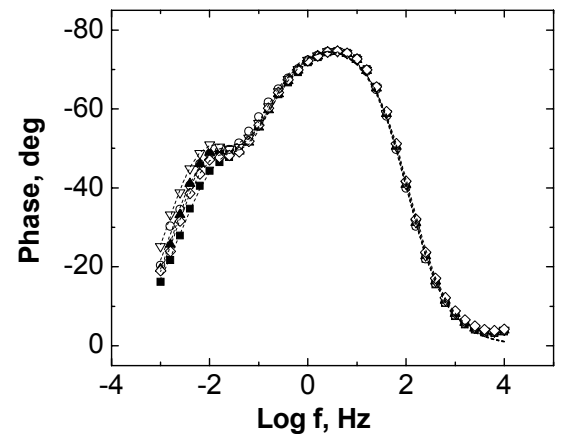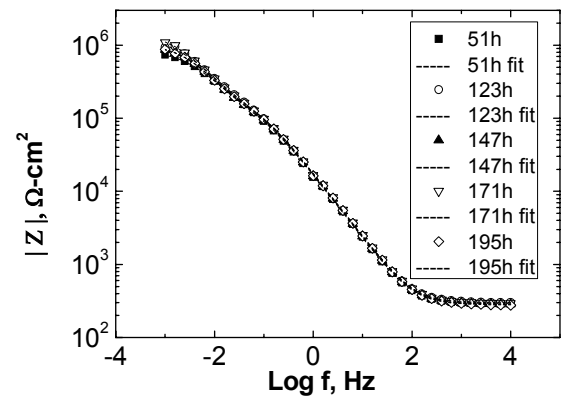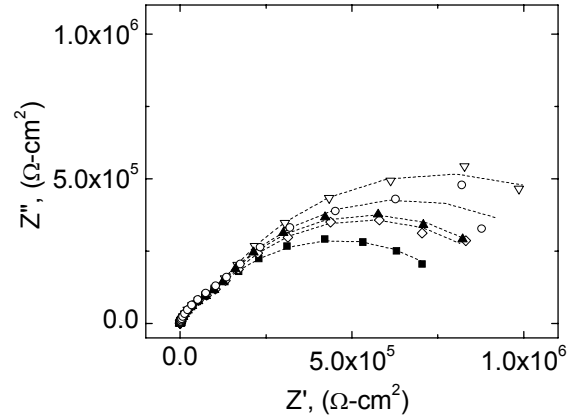
Fig. 7. Nyquist and Bode plots of the experimental data for SS and simulated spectra according to the model of Fig. 6, a

Table 2. EIS data simulation for the coated and uncoated samples

Sample/ Time, h	R_s, Ωcm^2	R_2, MΩcm^2	R_1, kΩcm^2	Q_2, μFcm^2	n	Q_1, μFcm^2	m
SS							
51	285.1	0.725	149	18.9	0.74	11.5	0.88
123	299.7	1.028	201	20.9	0.79	11.4	0.87
195	277.5	0.815	194	25.7	0.82	11.5	0.87
Ti 100							
51	298.0	0.076	74.4	80.5	0.94	36.3	0.82
123	308.7	0.170	0.63	11.8	0.77	19.7	0.90
195	310.1	1.171	0.53	13.9	0.68	16.4	0.92
Ti 530							
51	173.9	1.079	209	63.3	0.84	37.8	0.82
123	171.9	2.494	198	61.2	0.89	34.6	0.82
195	183.2	11.21	254	46.2	0.91	28.5	0.81
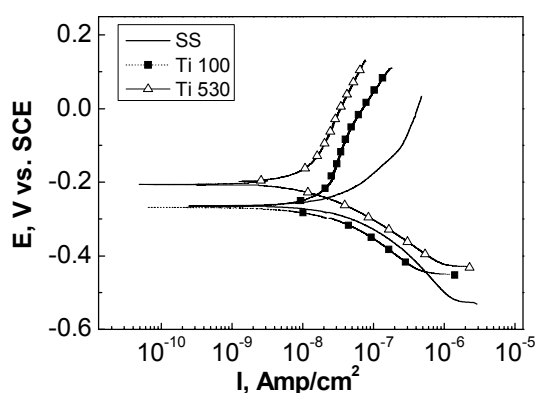
Fig. 8. Polarization curves for SS, Ti 100 and, T1 530 in NaCl 0.89 %. Scan rate is 0.1666mV/s

Table 3. Parameters obtained from the polarization curves

Sample	E_{corr}, mV	i_{corr}, nA/cm^2	β_a, V/dec	β_c, V/dec	R_p, MΩcm^2
SS	−263	60.0	0.285	0.189	0.815
Ti 100	−267	28.1	0.920	0.139	1.690
Ti 530	−195	18.9	0.258	0.130	1.780

CONCLUSIONS

1. Ti thin films of various thicknesses differently protect SS immersed into NaCl 0.89 % solution, which can be related with the amount of permeable defects.
2. OCP values show an increase in the noble direction of the sample Ti 530, while SS exhibits a decrease with time. The sample Ti 100 behaves more like the SS up to 150 h, and show a slight increment of potential at 195 h.
3. The electrochemical behavior of Ti thin films on SS is described by the equivalent circuit with two time constants. The sample Ti530 show high values of the substrate polarization resistance while the sample Ti 100 does not show a benefit for the same parameter.
4. The corrosion resistance values on the coated samples can be attributed to the formation of the passive layer of titanium but, if the thin film contains a small amount of permeable defects, this combination retards the corrosion process with time.
5. The Ti 530 coating can have a beneficial and desired effect on corrosion behavior of stainless steel 316L decreasing the corrosion current density that is an advantage for preventing ion release in biomedical applications.

REFERENCES

1. **Mathieu, H. J., Mathieu, J. B., McClure, D. E., Landolt, D.** Beam Effects in Auger Electrón Spectroscopy Analysis of Titanium Oxide Films *Journal of Vacuum Science Technology* 14 (4) 1977: pp. 1023 – 1028.
2. **Ajagy, O. O., Soppet, M. J., Erdemir, A., Fenske, G. R.** Assessment of Amorphous Carbon Coating for Artifitial Joint Applications *Tribology & Lubriction Technology* 61 (10) 2005: pp. 40 – 48.
3. **Fonseca, C., Vaz, F., Barbosa, M. A.** Electrochemical Behavior of Titanium Coated Steels by r.f. Sputtering in Shyntetic Sweat Solutions for Electrode Applications *Corrosion Science* 46 2004: pp. 3005 – 3018.
4. **Acero, J., Calderón, J., Salmeron, J. I., Verdaguer, J. J., Concejo, C.** The Behavior of Titanium as a Biomaterial: Microscopy Study of Plates and Surrounding Tissues in Facial Osteosynthesis *Journal of Cranio-Maxillofacial Surgery* 27 1999: pp. 117 – 123.
5. **Franco, C. V., Fontana, L. C., Bechi, D., Martinelli, E., Muzart, J. L. R.** An Electrochemical Study of Magnetron-Sputtered Ti and TiN-coated Steel *Corrosion Science* 40 (1) 1998: pp. 103 – 112.
6. **Cesiulis, H., Baltrunas, G., Padgurskas, J.** The Effect of FOLEOX Thin Films on the Corrosion Behavior of Armco Iron *Materials Science* (*Medžiagotyra*) 8 (2) 2002: pp. 392 – 395.
7. **Cottis, R., Turgoose, S.** Electrochemical Impedance and Noise. Corrosion Testing Made Easy. NACE, 1999.
8. **Turcio-Ortega, D., Pandiyan, T., García-Ochoa, E. M.** Electrochemical Impedance Spectroscopy (EIS) Study of the Film Formation of 2-imidazoline Derivatives on Carbon Steel in Acid Solution *Materials Science* (*Medžiagotyra*) 13 (2) 2007: pp. 163 – 166.
9. **Pan, J., Thierry, D., Leygraf, C.** Electrochemical Impedance Spectroscopy Study of the Passive Oxide Film on Titanium for Implant Applications *Electrochimica Acta* 41 (7/8) 1996: pp. 1143 – 1153.
10. **Fathi, M. H., Salchi, M., Saatchi, A., Mortazavi, V., Moosavi, S. B.** In Vitro Corrosion Behavior of Bioceramic, Metallic, and Bioceramic-Metallic Coated Stainless Steel Dental Implants *Dental Materials* 19 2003: pp. 188 – 198.
11. **Nie, X., Leyland, A., Matthews, A.** Deposition of Layered Bioceramic Hydroxyapatite/TiO$_2$ Coatings on Titanium Alloys Using Hybrid Technique of Micro-arc Oxidation and Electrophoresis *Surface Coatings Technologies* 125 2000: pp. 407 – 414.
12. **Stern, M., Geary, A. L.** Electrochemical Polarization *Journal of the Electrochemical* Society 104 (1) 1957: pp. 56 – 63.